

Anisotropic phonon DOS: the application of Rietveld and Mössbauer texture analysis in aligned powders

A. I. Rykov,^{1,2,3} M. Seto,⁴ Y. Ueda,⁵ and K. Nomura²

¹*Siberian Synchrotron Radiation Center, Lavrentieva 11, Novosibirsk, 630090, Russia,* ²*The University of Tokyo, Hongo 7-3-1, 113-8656, Japan,*

³*Technology Crystals Laboratory "Tecrys", Institutskaya 4/1, 630090, Novosibirsk, Russia,* ⁴*Research Reactor Institute, Kyoto University, Noda, Kumatori-machi, Osaka 590-0494, Japan,* ⁵*Institute for Solid State Physics, University of Tokyo, 5-1-5, Kashiwanoha, Chiba 277-8581, Japan*

(Dated: November 23, 2018)

While synthesizing the single crystals of novel materials is not always feasible, orienting the layered polycrystals becomes an attractive method in the studies of angular dependencies of inelastic scattering of x-rays or neutrons. Putting in use the Rietveld analysis of layered structures in novel manganites and cuprates we develop the studies of their anisotropic properties with oriented powders instead of single crystals. Densities of phonon states (DOS) and atomic thermal displacements (ATD) are anisotropic in the A-site ordered manganites $\text{LnBaMn}_2\text{O}_y$ of both $y = 5$ and $y = 6$ series (Ln=Y, La, Sm, Gd). We establish the angular dependence of DOS on textures of arbitrary strengths, link the textures observed by x-ray and γ -ray techniques, and solve the problem of disentanglement of Goldanskii-Karyagin effect (GKE) and texture in Mössbauer spectra.

PACS numbers: 63.22.Np;76.80.+y

Two states of matter traditionally used in structure analysis are single crystals and polycrystalline powder. When synthesizing the single crystal is a stiff task the random polycrystalline materials or even polycrystals oriented on a surface conformably to their persistent crystal habitus can be employed. Via the method developed initially by Rietveld[1] the refinement of texture, or preferred orientation, is a conventional procedure alongside with the refinement of atomic structure parameters. Randomization of the powders favors the perfect refinements of atomic parameters, therefore, any residual texture is usually not in line with the best sample preparation for x-ray profile analysis. There appears, however, a class of problems, in which the well-oriented powders of platy or acicular crystallites can replace the unavailable single crystals. To them belong the studies in anisotropic properties of materials, in electric, magnetic properties, and in lattice dynamics. The texture descriptions and determination of the preferred orientation parameters are thus becoming the issues of self-sustained interest.

Recently, orienting powders to make the samples with varied degree of crystallite alignment was suggested[2] to be useful in vibrational spectroscopy of anisotropic materials. When the polycrystalline material is a ferromagnet or a superconductor it can be thoroughly subjected to texturing in an external magnetic field.

The vibrational properties in novel manganites and cuprates are anisotropic owing to their layered structure. Substitution of Fe into $3d$ Jahn-Teller cation site perturbs the electronic system at small doping rate, and modifies the existing charge and/or orbital order. However, due to strong electron-phonon interactions the system keeps its attractiveness for high-resolution spectroscopies based on nuclear γ -resonance. The Fe-doped samples allowed us

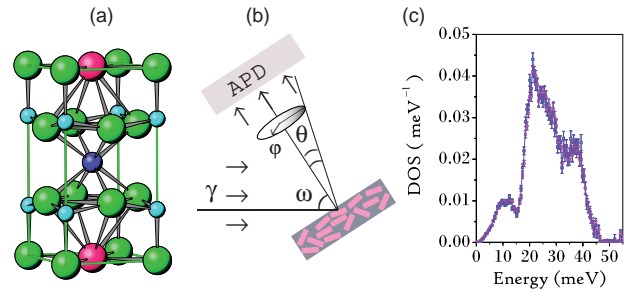


FIG. 1: Structure of oxygen-deficient layered oxides, e.g., manganites $\text{LnBaMn}_2\text{O}_5$ (a); geometry of nuclear inelastic scattering of synchrotron radiation (b); phonon density of states of Fe in unoriented powder of $\text{TbBaFe}_2\text{O}_5$ (c).

to probe the anisotropy of the dopant vibrations due to GKE in ^{57}Fe Mössbauer spectroscopy[3]. The same doping procedure is extremely valuable in the synchrotron radiation vibrational spectroscopy using the nuclear inelastic scattering (NIS) [4]. In this work, we establish the relationships between the parameters of preferred orientation, the anisotropic phonon DOS, and the Mössbauer line intensities. Using these relationships we propose the novel technique of NIS on the oriented powder samples.

Previous works dealt with the texture manifestations in Mössbauer spectra[5, 6, 7]. For a unpolarized Mössbauer source there occur two parameters of texture, which can be determined from spectra. These parameters define the so-called "minimum texture function" (MTF). Our approach is to employ the March-Dollase[8] function (MDF) implemented in programs for diffraction profile analysis[9, 10]. We establish the relation between

Rietveld and Mössbauer textures in terms of MDF and MTF, using the example of quadrupole doublet spectra for the ^{57}Fe nuclei occupying 2% of Mn sites in paramagnetic state of novel manganites $\text{LnBaMn}_2\text{O}_5$ [11] and $\text{LnBaMn}_2\text{O}_6$ [12, 13, 14]. The symmetries are tetragonal, except a monoclinic member YBaMn_2O_6 , and measurements were made with azimuthal rotation. Our texture function $T(\theta)$ was uniaxial, φ -invariant (Fig.1).

In the proposed method, the DOS derivation is based on two NIS patterns and a Rietveld pattern. Owing to relationship between MTF and MDF, the Mössbauer spectra and Rietveld analysis become mutually complementary techniques. Indeed, the transmission (Mössbauer) and reflection (Bragg or NIS) data may diverge if there occur some in-depth variations of texture. The γ -resonance wavelength (0.86 Å) is close to x-ray Mo K_α (0.7 Å), but the main component of NIS radiation collected by the avalanche photodiode detector (APD) is Fe K_α (1.94 Å)[4], that is close to x-ray wavelength of Cu K_α (1.54 Å).

In the NIS spectrum of an anisotropic crystal, the phonon DOS is weighted by squared projection of the phonon polarization vectors to the wave vector of the x-ray quantum[15]. Let the incident beam be launched under the angle ϑ with respect to preferred axis (z -axis) of a plate- or a needle-like crystallite. The projected DOS for this crystallite is:

$$g_E(\vartheta) = g_z(E) \cos^2 \vartheta + g_x(E) \sin^2 \vartheta \quad (1)$$

To introduce the averaging of the DOS over the ensemble of aligned crystallites we must integrate these two terms with the volume of crystallites $D(\vartheta, \phi)d\Omega$ whose z -axis lies within the cone shell element $d\Omega$:

$$\langle g(E) \rangle = g_x(E) + \Delta g_{zx}(E) \int D(\vartheta, \phi) \cos^2 \vartheta d\Omega \quad (2)$$

Here $\Delta g_{zx}(E) = g_z(E) - g_x(E)$ and the orientation distribution function (ODF) is normalized to unity. The polar ODF $T(\theta)$ is to replace $D(\vartheta, \phi)$ via the coordinate transform from the frame of the beam to the frame of the rotation stage. The ratio of angular elements $d\Omega_{\text{beam}}/d\Omega_{\text{stage}}$ is $\sin \vartheta d\vartheta d\phi / \sin \theta d\theta d\varphi$ and the Jacobian of this transform is $\sin \vartheta / \sin \theta$. Using $\cos \vartheta = \cos \theta \cos \omega - \sin \theta \sin \omega \cos \varphi$ we obtain for the uniaxial symmetry

$$\langle \cos^2 \vartheta \rangle = \langle \cos^2 \theta \rangle \cos^2 \omega + \frac{1}{2} \langle \sin^2 \theta \rangle \sin^2 \omega \quad (3)$$

Powder averaging $\langle \sin^2(\theta) \rangle = \int \sin^2(\theta) T(\theta) \sin \theta d\theta$ can be expressed via Legendre function of the first kind $P_2(x) = \frac{1}{2}(3x^2 - 1)$:

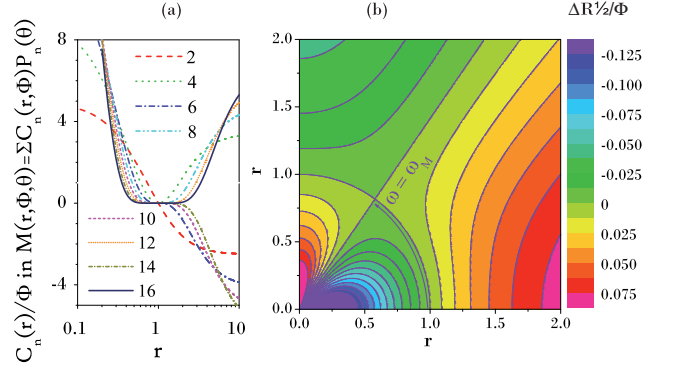


FIG. 2: The r -dependence of the Φ -scaled coefficients of the Legendre series expansion of the MDF, Eq. 6 (a) and contour polar plot of the isotropic ($\alpha = 0$) site Φ -scaled spectra asymmetry $\Delta R_{\perp}/\Phi$ in function of the strength of preferred orientation r and incidence angle ω (b).

$$\langle \sin^2 \theta \rangle = \frac{1}{3} \int_{-\pi/2}^{\pi/2} T(\theta) [P_2(\cos \theta) - 1] d(\cos \theta) \quad (4)$$

Prior measuring the NIS spectra Mössbauer spectroscopy and Rietveld analysis provide the results in terms of MTF and MDF, respectively. Due to the axial symmetry, the texture function $T(\theta)$ would have only even terms in the Legendre expansion series.

$$T(\theta) = \frac{2n+1}{2} \sum_{n=0}^{\infty} C_n P_n(\cos \theta) \quad (5)$$

The observable quantities, $\langle g(E) \rangle$, and asymmetries in Mössbauer spectra (R or ΔR_{\perp} , as denoted below) are fully determined by the integrals of $T(\theta)$, i.e., (4) and $\langle \cos^2 \theta \rangle = 1 - \langle \sin^2 \theta \rangle$, therefore, the function $T(\theta)$ consistent with experiment is not unique. The simplest function $T(\theta)$ conforming the Eq. (4), is the so-called MTF [6], composed of a linear combination of $P_0 = 1$ and $P_2(\cos \theta)$ terms, i.e., the parabolic function of $\cos \theta$.

Rietveld analysis[1, 9, 10] specifies the preferred orientation with two fit parameters r and Φ of the MDF [8]:

$$M(\theta, \Phi, r) = 1 - \Phi \left[1 - (r^2 \cos^2 \theta + r^{-1} \sin \theta)^{-\frac{3}{2}} \right] \quad (6)$$

The angle θ describes the misfit of the crystallite orientation with respect to the axis of the uniaxial texture (Fig.1, b), and Φ is the fraction of the oriented phase. The March variable r expresses the strength of the preferred orientation. In a sample made by pressing a layer of plates (needles) of the initial thickness d_0

(d) down to the thickness d (d_0), the degree of compression is $r = d/d_0$ [16]. The function $M(\theta, \Phi, r)$ conserves the scattering matter, therefore, it has a clearer physical sense than $T(\theta)$ originally used by Rietveld $T(\theta) = \exp(-r \cdot \theta^2)$ [1]. MDF is thus a true normalized angular distribution, equally good to the textures made of crystallites with either platy or acicular habitus[1, 9, 10].

Ericsson and Wappling have previously studied in chlorite[16] the effect of texturing induced by compression of various degrees $r_i = d_i/d_0$ on the Mossbauer line area asymmetry. They have pointed out that their model "represent an extreme case" and that less randomness were observed in chlorite samples than predicted by their one-parametric compression model. Nagy [17] has introduced a second parameter taking into account the particle shape and assumed that the texturing behavior of the particles under compression is shape-dependent. For the platy chlorite flakes Nagy obtained the aspect ratio (cylindrical h/D) as large as 0.6 [17]. The March-Dollase function implemented in the FULLPROF program[10] is also two-parametric, however, the meaning of the second parameter Φ is unrelated to the method of particle alignment. The unaligned random phase is just added with the fraction of $1 - \Phi$. We show below that the Mossbauer line area asymmetry depends for small asymmetries only on the product Φr . Difference of physical meanings between Φ and r manifests itself only in strongly asymmetric spectra.

Measurements with the rotated sample stage inclined to the incident beam (Fig.1, b) provide us with two components $g_x(E)$, $g_z(E)$ of uniaxial DOS in terms of the angle ω and the parameters r and Φ . Using MDF (Eq.6), we obtain

$$\langle \sin^2 \theta \rangle \equiv V(r, \Phi) = \int_0^1 M(\theta, \Phi, r) \sin^3 \theta d\theta \quad (7)$$

$$V(r, \Phi) = \frac{2}{3}(1 - \Phi) + \Phi v(r) \quad (8)$$

$$v(r) = \frac{r^2}{\varepsilon^2(r)} - \frac{\beta(r)}{2\varepsilon^3(r)} \quad (9)$$

$$\varepsilon(r) = \sqrt{r^2 - r^{-1}} \quad (10)$$

$$\beta(r) = \ln(2r^3 + 2\sqrt{r^6 - r^3} - 1) \quad (11)$$

$$\langle \cos^2 \vartheta \rangle = [1 - V(r, \Phi)] \cos^2 \omega + \frac{V(r, \Phi)}{2} \sin^2 \omega \quad (12)$$

via substitution $\langle \sin^2 \theta \rangle$, $\langle \cos^2 \theta \rangle$ into Eq.(3). Both $\varepsilon(r)$ and $\beta(r)$ are imaginary for $0 < r < 1$, however, $v(r)$ is real for $0 < r < \infty$. The ranges $0 < r < 1$, and $1 < r < \infty$ correspond to platy and stalky habits, respectively.

Now from (5) we can express MTF through r and Φ :

$$\frac{C_0}{2} + \frac{5}{2}C_2P_2(x) = \left(\frac{15}{4} - \frac{45}{4}x^2\right) V(r, \Phi) + \frac{15}{2}x^2 - \frac{3}{2} \quad (13)$$

It is shown in Fig.2 (a) that the Legendre series coefficients of the MDF are (all, except $C_0 = 1$) returning to

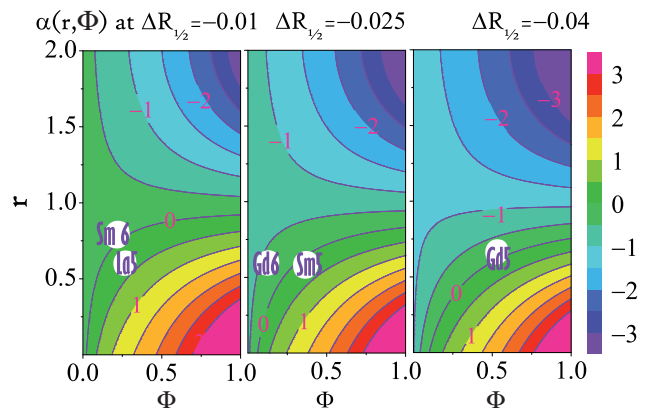


FIG. 3: Vibrational anisotropy $\alpha = k^2(\langle z^2 \rangle - \langle x^2 \rangle)$ in function of three variables $\alpha(r, \Phi, \Delta R_{\frac{1}{2}})$, Eq. 22, is shown as three slices (contour plots) of $\alpha(r, \Phi)$. In each $\Delta R_{\frac{1}{2}}$ -matched slice, the oriented samples of manganites $\text{LnBaMn}_2\text{O}_5$ and $\text{LnBaMn}_2\text{O}_5$ are shown by Ln symbols and oxygen index as spots with coordinates r, Φ obtained from Rietveld refinement of parameters of preferred orientation.

zero at $r = 1$ and that the MDF is well approximated by $\frac{1}{2}C_0 + (5/2)C_2P_2(x)$ in some vicinity of random polycrystal ($r = 1$), because $C_n \simeq 0$ for $n \geq 2$ around $r = 1$.

We are ready for determination of both $g_x(E)$ and $g_z(E)$. From Eq.(2) a couple of measurements of DOS $g_1(E)$ and $g_2(E)$ at the angles ω_1 and ω_2 leads to:

$$\Delta g_{zx}(E) = \frac{\Delta g_{12}(E)}{\left[1 - \frac{3}{2}V(r, \Phi)\right] (\cos^2 \omega_1 - \cos^2 \omega_2)} \quad (14)$$

$$g_x(E) = \bar{g}(E) - \frac{\Delta g_{12}(E)}{2} \frac{(\cos^2 \omega_1 + \cos^2 \omega_2)}{(\cos^2 \omega_1 - \cos^2 \omega_2)} \quad (15)$$

$$\bar{g}(E) = g_1(E)/2 + g_2(E)/2, \quad \Delta g_{12}(E) = g_1(E) - g_2(E).$$

Now we turn to the asymmetry of Mossbauer spectra caused by texture with parameters r and Φ . First, the intensity ratio for a single crystallite is to be examined depending on the orientation of the wave vector of the incident x-ray quantum with respect to the axes of the electric field gradient (EFG) tensor at the site wherein the ^{57}Fe nucleus is located. The ϑ -dependent Clebsch-Gordan coefficients determine the doublet line intensity ratio R [5, 6]. We found that the quantity, which is proportional to the amount of the oriented phase Φ is the deviation of relative line area from 1/2:

$$\Delta R_{\frac{1}{2}} = \frac{I_{\pm\frac{1}{2} \rightarrow \pm\frac{1}{2}} - I_{\pm\frac{3}{2} \rightarrow \pm\frac{1}{2}}}{2(I_{\pm\frac{1}{2} \rightarrow \pm\frac{1}{2}} + I_{\pm\frac{3}{2} \rightarrow \pm\frac{1}{2}})} = \frac{1}{8}(1 - 3 \cos^2 \vartheta) \quad (16)$$

Powder averaging resolves, using Eq.(3), into

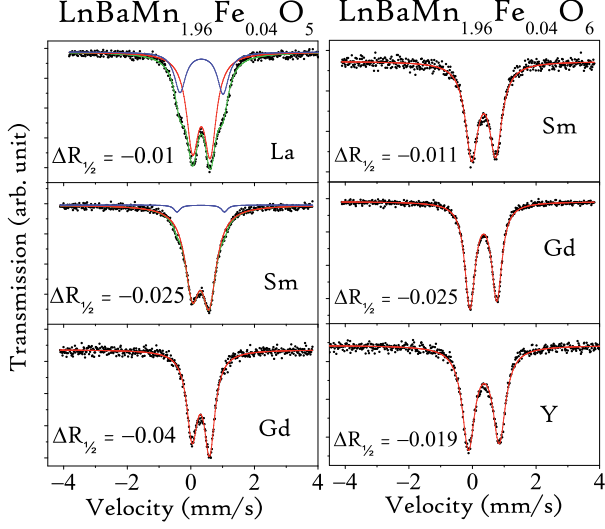


FIG. 4: Mössbauer spectra in oriented samples of ^{57}Fe -doped manganites. Two panels present the oxygen-poor and oxygen-rich series ("O₅" and "O₆"). The spectra are fitted either with one or with two asymmetric doublets. Meltdowns of $\text{Mn}^{2+}/\text{Mn}^{3+}$ and $\text{Mn}^{3+}/\text{Mn}^{4+}$ charge order in O₅ and O₆ series, respectively, are seen as single-site doublets. The occurrence of two sites for Fe in La and Sm members of the $\text{LnBaMn}_2\text{O}_5$ series is interpreted as remainder of unmolten charge order between Mn^{2+} and Mn^{3+} . The asymmetries $\Delta R_{\frac{1}{2}}$ were fixed to be a single parameter of both doublets. This is because each crystallite contain both these sites and their V_{zz} direction and sign coincide according to structure[11].

$$\Delta R_{\frac{1}{2}} = \frac{3}{8}V(r, \Phi) - \frac{1}{4} + \left[\frac{3}{8} - \frac{9}{16}V(r, \Phi) \right] \sin^2 \omega \quad (17)$$

Eq.(17) remains true in Φ -scaled form, i.e. with $\Delta R_{\frac{1}{2}}/\Phi$ in place of $\Delta R_{\frac{1}{2}}$, and $v(r)$ in place of $V(r, \Phi)$. From Fig. 2(b) starting with $\Delta R_{\frac{1}{2}}/\Phi$ one finds the MDF variable r at any angle ω except magic angle $\omega_M = 54.7^\circ$.

When the measurement is done at $\omega = \omega_M$ the texture does not manifest itself in the spectra. In a simple normal incidence transmission Mossbauer spectrum ($\omega = 0$), the expression for intensity ratio was formulated[5],

$$R = \frac{\int_0^{\pi/2} M(\theta, \Phi, r)(1 + \cos^2 \theta)e^{-\alpha \cos^2 \theta} d\theta}{\int_0^{\pi/2} M(\theta, \Phi, r)(2/3 + \sin^2 \theta)e^{-\alpha \cos^2 \theta} d\theta} \quad (18)$$

however, the solutions were yet found either for texture effects, or for GKE, separately only. In the proposed synchrotron experiments on anisotropic powders, both are crucial, therefore, the combined effects of texture and GKE are of our interest. In (18) α is the squared wave

vector times the difference of mean-square vibrational displacements along V_{zz} , and in perpendicular direction, $\alpha = k^2(\langle z^2 \rangle - \langle x^2 \rangle)$, $k^2 = 53.35\text{\AA}^{-2}$. Here again, it is more convenient to work with $\Delta R_{\frac{1}{2}} = \frac{1}{2}(1 - R)/(1 + R)$. The replacement of $M(\theta, \Phi, r)$ with the MTF, Eq. 13, makes our expression for $\Delta R_{\frac{1}{2}}$ integrable and expressible via two simple sigmoid functions $\sigma_0(\alpha)$ and $\sigma_1(\alpha)$:

$$\Delta R_{\frac{1}{2}} = \frac{\sigma_0(\alpha) + \Phi U(r) \left[\frac{15}{2}\sigma_1(\alpha) - 5\sigma_0(\alpha) - \frac{5}{8} \right]}{1 - 20\Phi U(r)\sigma_0(\alpha)} \quad (19)$$

with $U(r) = 1 - 3v(r)/2$, $\sigma_1(\alpha) = (1 + 3/2\alpha)\sigma_0(\alpha)$, and

$$\sigma_0(\alpha) = \frac{1}{8} - \frac{3}{16\alpha} \left(1 - \frac{e^{-\alpha}}{K(\alpha)} \right) \quad (20)$$

Here $K(\alpha) = {}_1F_1(\frac{1}{2}, \frac{3}{2}, -\alpha)$ is the Kummer confluent hypergeometric function. The range of variation for both sigmoid functions $\sigma_0(\alpha)$ and $\sigma_1(\alpha)$ is between $-1/4$ and $+1/8$; for unoriented powder $r = 1$, $v(1) = 0$, and $\Delta R_{\frac{1}{2}}(\alpha) = \sigma_0(\alpha)$ is the exact solution. The accuracy of the solution (19) is better than 1% only in the narrow range of slight textures ($0.9 \lesssim r \lesssim 1.1$ and $0 \leq \Phi \leq 1$), in which the MTF is a perfect approximation for MDF (Eq. 6). In the same range, the $\Delta R_{\frac{1}{2}}(\alpha)$ differs from $\sigma_0(\alpha)$ merely by shift of sigmoid flexpoint:

$$\Delta R_{\frac{1}{2}}(r, \Phi, \alpha) = \sigma_0(\alpha - \alpha_0(r, \Phi)) \quad (21)$$

The approximation (21) is as good as (19) for $\alpha_0 = 4.53(1 - \Phi r)$. The parameters r and Φ enter to α_0 in equivalent form, however, become nonequivalent if the σ_0 -approximation (21) is extended to a broader range of r . We extend it by taking into account the narrowing sigmoid for stronger textures: $\Delta R_{\frac{1}{2}}(r, \Phi, \alpha) = \sigma_0(A(r, \Phi)\alpha - B(r, \Phi))$. The accuracy of this approximation is better than 1% in the broad range of textures, $0.3 \lesssim r \lesssim 2$. The r and Φ dependencies of A and B can be well fitted with $A(r, \Phi) = 1 + \Phi A_1(r) + \Phi^2 A_2(r) + \Phi^3 A_3(r)$ and $B(r, \Phi) = \Phi B_1(r) + \Phi^2 B_2(r) + \Phi^3 B_3(r)$. The polynomials $A_i(r)$ and $B_i(r)$ could be expressed as dot products of coefficients vectors $(a_0, a_1, a_2, a_3, a_4)_i$ with the vector $(1, r, r^2, r^3, r^4)$ [18]. In practice, it is crucial to find the vibrational anisotropy α starting from $\Delta R_{\frac{1}{2}}$, therefore, α is given using the function inverse of σ_0 :

$$\alpha(r, \Phi, \Delta R_{\frac{1}{2}}) = \frac{\sigma_0^{-1}(\Delta R_{\frac{1}{2}})}{A(r, \Phi)} + \frac{B(r, \Phi)}{A(r, \Phi)} \quad (22)$$

The function of 3 variables $\alpha(r, \Phi, \Delta R_{\frac{1}{2}})$ is visualized via several 2D maps (slices, Fig.3). Total range, in which $\sigma_0^{-1}(\Delta R_{\frac{1}{2}})$ is defined, is $-0.25 < \Delta R_{\frac{1}{2}} < 0.125$, and the slices are shown for $\Delta R_{\frac{1}{2}} = -0.01, -0.025, \text{ and } -0.04$. Linear slope $\sigma_0^{-1} = 30\Delta R_{\frac{1}{2}}$ is exact near $\Delta R_{\frac{1}{2}} \simeq 0$, but

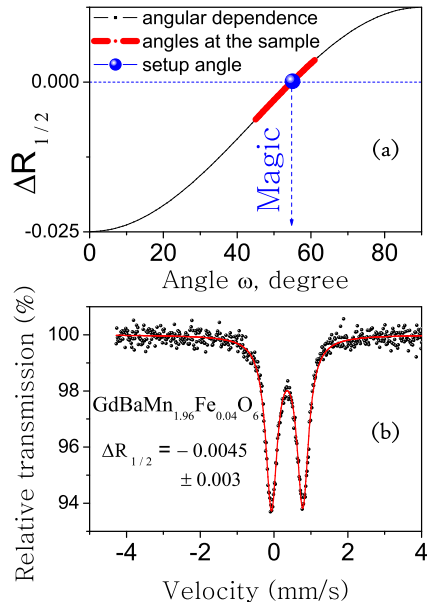


FIG. 5: The angular dependence of the doublet asymmetry (a) as given by the Eq. (17) and the Mössbauer spectrum measured under the magic angle $\omega_M = 54.7^\circ$ between the direction from source to detector and the normal to the $\text{GdBaMn}_{1.96}\text{Fe}_{0.04}\text{O}_6$ sample absorber. The distance between source and the sample center was $L = 4$ cm and the illuminated area of the sample was 2×2 cm ($d \times d$). The angles at the absorber surface were thus varied between $\omega_1 = \omega_M - \tan^{-1}\left(\frac{d \cos \omega_M}{L - d \sin \omega_M}\right)$ and $\omega_2 = \omega_M + \tan^{-1}\left(\frac{d \cos \omega_M}{L + d \sin \omega_M}\right)$. This range between $\omega_1 = 45^\circ$ and $\omega_2 = 61^\circ$ is shown in (a) by bold line. A small residual asymmetry might have been resulted from the averaging in this range. The fitted value of $\Delta R_{1/2} = 0.0045$ is 5.5 times smaller than the normal-incidence value of $\Delta R_{1/2}$ in Fig.4.

its discrepancy reaches 10% already at $\Delta R_{\frac{1}{2}} = -0.05$. The parabolic model $\sigma_0^{-1} = 31.4\Delta R_{\frac{1}{2}} + 96.5\Delta R_{\frac{1}{2}}^2$ is better than 0.1% in the range $-0.05 < \Delta R_{\frac{1}{2}} < 0.05$ that covers the asymmetries observed in our spectra (Fig.4).

We have checked that the rotation of the sample around an axis perpendicular to the \vec{k} -vector of the incident γ -quantum induces a difference of the doublet asymmetry. The same as in Fig.4 absorber of $\text{GdBaMn}_{1.96}\text{Fe}_{0.04}\text{O}_6$ was installed under the magic angle $\omega_M = 54.7^\circ$ and the symmetric doublet was obtained. A very small residual asymmetry can be explained by the divergence of the incident beam (Fig.5).

Both oxygen-saturated and oxygen-depleted families of layered manganites show negative $\Delta R_{\frac{1}{2}}$, although their left-to-right area ratio changes the sign between "O₅" and "O₆" series. This is because the main axis of EFG (z) is perpendicular to layers and $V_{zz} > 0$ in the pyramid

FeO_5 , but $V_{zz} < 0$ in the FeO_6 octahedron compressed along z -axis. Since the sign of V_{zz} changes from "O₅" to "O₆" series the doublet lines swap their positions. $\Delta R_{\frac{1}{2}}$ remains negative according to its definition in Eq.(16). Therefore, in both panels of Fig.4, the stronger line is $\pm 3/2 \rightarrow \pm 1/2$, and the weaker line is $\pm 1/2 \rightarrow \pm 1/2$. In this respect, the layered manganites are quite similar to layered cuprates, wherein the ionic point charge model prescribes the same orientation and sign of V_{zz} [19].

The values of r and Φ for our samples[20] refined from x-ray diffraction patterns[10] are shown by spots in Fig.3, at slices of the same $\Delta R_{\frac{1}{2}}$ as shown in Fig.4. The value of α increases with increasing size of Ln within either "O₅" or "O₆" series, however, the vibrational anisotropy is positive in pyramid FeO_5 ($\langle z^2 \rangle > \langle x^2 \rangle$), but negative in the compressed octahedron FeO_6 ($\langle z^2 \rangle < \langle x^2 \rangle$). This result is verifiable via refinement of the factors of anisotropic thermal displacements (ATD) of Mn from neutron diffraction data, however, till now such the data were refined with B_{iso} -models[13, 14]. On the other hand, in a similar bilayered structure of YBaFeCuO_5 , the ATD of Fe shaped in FeO_5 pyramid as prolate 'cigar' was found[21]. Also, the oblate 'pancake' is not unexpected shape of ATD in the oblate octahedron of $\text{LnBaMn}_2\text{O}_6$.

In conclusion, we have shown how the information contained in the x-ray diffraction full-profile patterns of the aligned powders can be used for finding the direction-projected components of the phonon DOS. This information is sufficient, in principle, to solve the problem of determination of two DOS components from at least two experiments either performed on two samples with different and non-zero degrees of alignment or conducted on one aligned-powder sample but under at least two different angles ω . The same information is contained in asymmetry of Mössbauer line intensities, however, here the texture effect is entangled with GKE. Therefore, the useful for DOS or for other properties information can be disentangled from Mössbauer spectra in only cases when either GKE or ODF are characterized by some separate experiments. One possibility is to determine the GKE separately from the ATD refinement using neutron diffraction full-profile analysis superior in the accuracy of B_{aniso} compared to x-ray Rietveld analysis. Another possibility is to employ the texture March-Dollase parameters. The latter possibility was realized in this work for two cases when the sign and orientation of uniaxial V_{zz} is known, namely, in $\text{LnBaMn}_2\text{O}_5$ ($V_{zz} > 0$) and in $\text{LnBaMn}_2\text{O}_6$ ($V_{zz} < 0$). Our method is well applicable for these tetragonal structures, in which the axis of preferred orientation coincides with the direction perpendicular to layers and with the principal axis of electric field gradient. More complicated textured systems, such as non-uniaxial or magnetic textures were beyond the scope of the present work. It must be finally emphasized that the scope of possible applications of the present work is limited by the close correspondence be-

tween the distribution of March-Dollase, which is theoretically substantiated only in pressed samples[17], and the real ODF $T(\theta)$, which can be obtained experimentally with texture goniometers using several analytical methods, best of which combine the ODF calculation with the Rietveld structure refinement[22]. Our approach is also good for samples containing the randomly oriented phase, because we employed the extended (biparametric) MDF $M(\theta, \Phi, r)$.

This work was supported by Asahi Glass Foundation and RFBR-JSPS (Grant 07-02-91201).

Solid Films **450** (2004) 34-41.

FIGURE CAPTIONS

Fig.1. Structure of oxygen-deficient layered oxides, e.g., manganites $\text{LnBaMn}_2\text{O}_5$ (a); geometry of nuclear inelastic scattering of synchrotron radiation (b); phonon density of states of Fe in unoriented powder of $\text{TbBaFe}_2\text{O}_5$ (c).

Fig.2. The r -dependence of the Φ -scaled coefficients of the Legendre series expansion of the MDF, Eq. 6 (a) and contour polar plot of the isotropic ($\alpha = 0$) site Φ -scaled spectra asymmetry $\Delta R_{\frac{1}{2}}/\Phi$ in function of the strength of preferred orientation r and incidence angle ω (b).

Fig.3. Vibrational anisotropy $\alpha = k^2(\langle z^2 \rangle - \langle x^2 \rangle)$ in function of three variables $\alpha(r, \Phi, \Delta R_{\frac{1}{2}})$, Eq. 22, is shown as three slices (contour plots) of $\alpha(r, \Phi)$. In each $\Delta R_{\frac{1}{2}}$ -matched slice, the oriented samples of manganites $\text{LnBaMn}_2\text{O}_5$ and $\text{LnBaMn}_2\text{O}_5$ are shown by Ln symbols and oxygen index as spots with coordinates r, Φ obtained from Rietveld refinement of parameters of preferred orientation.

Fig.4. Mossbauer spectra in oriented samples of ^{57}Fe -doped manganites. Two panels present the oxygen-poor and oxygen-rich series ("O₅" and "O₆"). The spectra are fitted either with one or with two asymmetric doublets. Meltdowns of $\text{Mn}^{2+}/\text{Mn}^{3+}$ and $\text{Mn}^{3+}/\text{Mn}^{4+}$ charge order in O₅ and O₆ series, respectively, are seen as single-site doublets. The occurrence of two sites for Fe in La and Sm members of the $\text{LnBaMn}_2\text{O}_5$ series is interpreted as remainder of unmolten charge order between Mn^{2+} and Mn^{3+} . The asymmetries $\Delta R_{\frac{1}{2}}$ were fixed to be a single parameter of both doublets. This is because each crystallite contain both these sites and their V_{zz} direction and sign coincide according to structure[11].

Fig.5. The angular dependence of the doublet asymmetry (a) as given by the Eq. (17) and the Mössbauer spectrum measured under the magic angle $\omega_M = 54.7^\circ$ between the direction from source to detector and the normal to the $\text{GdBaMn}_{1.96}\text{Fe}_{0.04}\text{O}_6$ sample absorber. The distance between source and the sample center was $L = 4$ cm and the illuminated area of the sample was 2×2 cm ($d \times d$). The angles at the absorber surface were thus varied between $\omega_1 = \omega_M - \tan^{-1}(\frac{d \cos \omega_M}{L - d \sin \omega_M})$ and $\omega_2 = \omega_M + \tan^{-1}(\frac{d \cos \omega_M}{L + d \sin \omega_M})$. This range between $\omega_1 = 45^\circ$ and $\omega_2 = 61^\circ$ is shown in (a) by bold line. A small residual asymmetry might have been resulted from the averaging in this range. The fitted value of $\Delta R_{1/2} = 0.0045$ is 5.5 times smaller than the normal-incidence value of $\Delta R_{1/2}$ in Fig.4.

-
- [1] H.M. Rietveld, J. Appl. Cryst. **2**, 65-71 (1969).
 - [2] A. I. Rykov, Europhys. Lett. **85**, 16003, p1-p6 (2009).
 - [3] A. Rykov, V. Caignaert, and B. Raveau, J. Solid. St. Chem. **109**, 295-306 (1994).
 - [4] M. Seto, Y. Yoda, S. Kikuta, X.W. Zhang and M. Ando, Phys. Rev. Lett. **74**, 3828-3831 (1995).
 - [5] H.-D. Pfannes and U. Gonser, Appl. Phys. **1**, 93-102 (1973).
 - [6] H.-D. Pfannes and H. Fisher, Appl. Phys. **13**, 317-325 (1977).
 - [7] J.-M. Greneche and F. Varret, J. Phys. **C15**, 5333-5344 (1982).
 - [8] W.A. Dollase, J. Appl. Cryst. **19**, 267-272 (1986).
 - [9] R.A. Young and D.B. Wiles, Adv.X-ray Anal. **24**, 1-23(1981).
 - [10] J. Rodriguez-Carvajal. Physica **B 192**, 55-69 (1993); <http://www-llb.cea.fr/fullweb/powder.htm>.
 - [11] F. Millange, V. Caignaert, B. Domengès, B. Raveau, and E. Suard, Chem. Mater. **10**, 1974-1983 (1998).
 - [12] T. Nakajima, H. Kageyama, Y. Ueda, J. Phys. Chem. Solids, **63**, 913-916 (2002).
 - [13] T. Nakajima, H. Kageyama, H. Yoshizawa, K. Ohoyama, and Y. Ueda, J. Phys. Soc. Jpn. **72**, 3237-3242 (2003).
 - [14] A.J. Williams, J.P. Attfield, and S.A.T. Redfern, Phys. Rev. **B 72**, 184426-1-13 (2005).
 - [15] V.G. Kohn, A.I. Chumakov, R. Rüffer, Phys. Rev. B. **58**, 8437-8444 (1998).
 - [16] T. Ericsson and R. Wäppling, J. Phys. Colloque **C6**, 719-723 (1976).
 - [17] D.L. Nagy, Appl. Phys. **17**, 269-274 (1978).
 - [18] Best fits were obtained for the following coefficient vectors: $A_1=(4.34,-12.3, 12.5,-5.35, 0.84)$, $A_2=(-5.27, 16.1,-17.9, 8.52,-1.47)$, $A_3=(2.35,-7.85, 9.47,-4.89, 0.903)$, $B_1=(11.5,-24.4, 19.7,-8.22, 1.33)$, $B_2=(-7.79, 24.2,-26.4, 11.8,-1.77)$, $B_3=(8.44,-29.6, 36.5,-18.6, 3.20)$.
 - [19] A.I. Rykov, A. Ducouret, N. Nguyen, V. Caignaert, F. Studer and B. Raveau, Hyperfine Interact. **77** (1993) 277.
 - [20] Since the structure of YBaMn_2O_6 was monoclinic, the refinement of texture parameters was not applicable.
 - [21] A.W. Mombrú, K. Prassides, C. Christides, R. Erwin, M. Pissas, C. Mitros, and D. Niarchos, J. Phys.: Cond. Mat. **10**, 1247-1258 (1998).
 - [22] L. Lutterotti, D. Chateigner, S. Ferrari, J. Ricote, Thin